Journal of Statistical Physics, Vol. 54, Nos. 3/4, 1989

Asymptotic Degeneracy of the Transfer Matrix Spectrum for Systems with Interfaces: Relation to Surface Stiffness and Step Free Energy

V. Privman[1] and N. M. Švrakić[1]

Received July 18,1988

Two- and three-dimensional Ising-type systems are considered in the finite-cross-section cylindrical geometry. An interface is forced along the cylinder (strip in $2d$) by the antiperiodic or $+-$ boundary conditions. Detailed predictions are presented for the largest asymptotically degenerate set of the transfer matrix eigenvalues. For rough interfaces, i.e., for $0 < T < T_c$ in $2d$, $T_R < T < T_c$ in $3d$, the eigenvalues are split algebraically, and the spectral gaps are governed by the *surface stiffness coefficient*. For "rigid" interfaces, i.e., $0 < T < T_R$ in $3d$, the eigenvalues are split exponentially, with the gaps determined by the *step free energy*.

KEY WORDS: Phase transitions; surface tension; surface stiffness; step free energy; finite-size correlation lengths.

1. INTRODUCTION

The *transfer matrix* (TM) method has been extremely useful in calculating critical-point properties of a variety of $2d$ models.[1] Recent advances in large-scale computing and combination of the TM and Monte Carlo techniques have made applications to $3d$ systems feasible.[2,3] Away from criticality, the TM spectrum may yield information not only on the bulk thermodynamic quantities, but also on various *interfacial properties* (below T_c). For Ising-type systems with periodic boundary conditions the leading spectral gap for $T < T_c$ is related to the surface tension.[4,5] This feature will be considered in detail in Section 2, where we also introduce the general

[1] Department of Physics, Clarkson University, Potsdam, New York 13676.

0022-4715/89/0200-0735$06.00/0

formalism of the asymptotic degeneracy of the largest TM eigenvalues. Note that for the n-vector spin systems, the leading spectral gaps are determined by the helicity modulus.[6]

Although we focus on Ising-type models, our considerations are extendible to other scalar spin systems with several coexisting phases which are not related continuously (i.e., no Goldstone or spin-wave modes are possible). Thus, the phases will be separated by sharp interfaces (instead of diffuse Bloch walls). Specifically, we consider $2d$ and $3d$ Ising-type systems in the cylindrical geometry, with an interface induced by the $+-$ or antiperiodic (*ap*) boundary conditions. Recent studies[7-11] in $2d$ have revealed certain unexpected features of TM spectrum for nonperiodic boundary conditions. Our main $2d$ result, derived in Section 3 and further checked by solid-on-solid model and some exact calculations in Section 4, is that the spectral gaps for both $+-$ and *ap* boundary conditions are governed by the *surface stiffness coefficient*. The results are summarized by Eqs. (3.23)–(3.24).

In $3d$, below the roughening temperature T_R, we argue, in Section 5, that the spectral gaps are determined by the *step free energy*, as summarized by relations (5.14)–(5.17). For the $3d$ case with $T_R < T < T_c$, the spectrum is again related to the surface stiffness coefficient. These results, relations (6.2)–(6.3), are presented in Section 6, which also contains some concluding remarks.

Our study does not include consideration of the scaling forms *at* T_R and T_c, where $T_R = 0$ in $2d$, $T_R > 0$ for lattice $3d$ models.[12] For noncritical temperature values, our relations provide a new method of estimating the surface stiffness coefficient and the step free energy by numerical TM calculations.

2. GENERAL FORMALISM. SYSTEMS WITH PERIODIC BOUNDARY CONDITIONS

In order to introduce the notation in a more familiar and relatively well-studied framework, as well as to discuss certain finite-size effects for later use, we consider first the case of the *periodic boundary conditions*. In $d \geqslant 2$ dimensions, we consider $L^{d-1} \times \infty$ cylinders at fixed temperature in the range $0 < T < T_c$. Here L is a linear size of the cross section, of area

$$A \equiv L^{d-1} \tag{2.1}$$

The cylinder partition function can be evaluated by building it up from slices of fixed microscopic length b along the infinite direction: In each

application of the TM a slice of volume bA is added in a standard fashion. The eigenvalues of the TM will be denoted Λ_j, with

$$\Lambda_0 > \Lambda_1 > \Lambda_2 > \cdots \tag{2.2}$$

Some of the eigenvalues may be multiply degenerate.

The *free energy density* of the cylinder, measured in units of $k_B T$, is given by

$$f(L) \equiv -(bA)^{-1} \ln \Lambda_0 \tag{2.3}$$

where $f(L)$ also depends on T and possibly on the cross-section *shape*. (Typically, we will display only the size dependences of various quantities.) We do not necessarily assume hypercubic shapes. Thus, (2.1) can be considered as a definition of L. However, we assume that the cross-section shape is fixed, while L is varying and large as compared to all the microscopic (lattice) lengths. For periodic boundary conditions the size dependence is weak,[13]

$$f(L) - f(\infty) \sim \exp(-L/\xi_\parallel) \tag{2.4}$$

Here $\xi_\parallel$ is some length of the order of the bulk single-phase correlation length.

Finite-size correlation lengths corresponding to the spectral gaps can be introduced via

$$\xi_j(L) = b[\ln(\Lambda_0/\Lambda_j)]^{-1} \tag{2.5}$$

where $j = 1, 2, \ldots$. The buildup of a phase transition is typically accompanied by the divergence, as $L \to \infty$, of one or more of the correlation lengths $\xi_j(L)$. The first-order transition (phase coexistence) buildup in the periodic Ising-type cylinder is associated with exponential divergence[4,5] of $\xi_1(L)$ only. The other extreme is represented, e.g., by the critical point spectrum, where an unbounded number of $\xi_j(L)$ diverge linearly with L.[1]

Generally, relations (2.3) and (2.5) yield the following form for the diagonal representation of the TM,

$$e^{-bAf(L)} \operatorname{diag}[1, e^{-b/\xi_1(L)}, e^{-b/\xi_2(L)}, \ldots] \tag{2.6}$$

(Here entries corresponding to multiply degenerate eigenvalues must be appropriately repeated. We neglect this feature for simplicity.) The longest length scale of variation of some of the finite-system correlation functions is fixed by $\xi_1(L)$, where we assume that at least $\xi_1(L) \to \infty$ as $L \to \infty$. Calculation of such correlations involves the TM raised to the power of

order ξ_1/b, i.e., applied $\sim \xi_1/b$ times. In the diagonal representation, the ξ_1/b power of the TM is

$$e^{-\xi_1 Af}\,\mathrm{diag}[1,\ 1/e,\ e^{-\xi_1/\xi_2},\ e^{-\xi_1/\xi_3},\ldots] \tag{2.7}$$

As $L \to \infty$, only the entries corresponding to the subset of ξ_j $(j \geqslant 2)$ such that the limits

$$\lim_{L\to\infty} [\xi_j(L)/\xi_1(L)] \tag{2.8}$$

are finite remain nonzero. Other entries in (2.7) vanish typically exponentially or faster as $L \to \infty$.

Unfortunately, the diagonal form of the TM is generally not known. The above heuristic arguments suggest, however, that there exists an *approximate* reduction of the TM to a subblock such that only the eigenvalues corresponding to the largest divergent finite-size length scales will be included. Thus, a subspace of the eigenstates asymptotically degenerate with the $j=0$ eigenstate is singled out. Such an effective TM can be constructed by phenomenological considerations.[5,6] It can range from a 2×2 matrix, e.g., for periodic Ising cylinders,[5] to an infinite-dimensional matrix (operator), e.g., for n-vector cylinders.[6] More generally, the size of the reduced TM can be L dependent: see, e.g., Section 5.

Several studies[2,4,5,7,10,11,14,15] suggest that for periodic Ising-type cylinders only the leading-gap correlation length $\xi_1(L)$ diverges as $L \to \infty$. A similar property is also true for *free* boundary conditions.[7,10,11,16] The predominant configurations of an $A \times \infty$ cylinder are alternating regions of $+$ or $-$ spontaneous magnetization, persisting over an average distance $\xi_1(L)$, separated by fluctuating interfaces running transverse to the infinite dimension (cylinder axis). The energy cost of one such interface is well approximated by $k_B T \sigma_\perp A$, where $\sigma_\perp$ is the bulk surface tension for transverse interfaces (interfacial free energy per unit hyperarea and per $k_B T$). Note that $\sigma_\perp$ and many other "constants" used below are actually T dependent. Consideration of the "dilute gas of interfaces" then yields[4,17] the large-L form

$$\xi_1(L) \approx \delta \exp[\tilde{\sigma}(L)\, A] \tag{2.9}$$

where δ is some microscopic length, while

$$\lim_{L\to\infty} \tilde{\sigma}(L) = \sigma_\perp \tag{2.10}$$

The interpretation of $\tilde{\sigma}(L)$ and the rate of convergence in (2.10) will be discussed shortly.

The diagonal representation of the reduced 2×2 TM is

$$e^{-bAf(L)}\,\mathrm{diag}[1, e^{-b/\xi_1(L)}] \tag{2.11}$$

Upon a 45° rotation, and expanding in b/ξ_1, keeping the leading-order terms only, this matrix can be put in a more symmetric form,

$$\{\exp[-bAf(L)]\}\begin{pmatrix} 1 & \dfrac{b}{2\delta}\exp[-\tilde{\sigma}(L)\,A] \\ \dfrac{b}{2\delta}\exp[-\tilde{\sigma}(L)\,A] & 1 \end{pmatrix} \tag{2.12}$$

This representation is reminiscent of the usual TM formulation. The prefactor in (2.12) is just the Boltzmann weight corresponding to the energy of a single-phase (+ or −) slice $b\times A$ added in one TM application. The nondiagonal terms contain an extra Boltzmann factor corresponding to the interaction energy, of order $k_B T\sigma_\perp A$, at the contacts of the + and − phases. This interpretation is obviously not rigorous. The result (2.12) is similar to the form used[5] in the studies of finite-size rounded first-order transitions, for which one also includes the magnetic energy in the diagonal matrix elements.[5]

Consider next the convergence rate in (2.10). Studies[18–21] of finite-size corrections for the interfacial free energy $\sigma(L)$ of interfaces of linear extent L in approximately cubic samples suggest that for large L,

$$\sigma(L)-\sigma(\infty)\approx L^{1-d}[\ln L + O(1)] \tag{2.13}$$

for *periodic* rough interfaces in general d, and

$$\sigma(L)-\sigma(\infty)\approx (2L)^{-1}\,[\ln L + O(1)] \tag{2.14}$$

for *free* (rough) interfaces in $d=2$. [For free boundary conditions in $d>2$, the leading finite-size correction is the (nonuniversal) $1/L$ term. We will not consider this case in detail here.] For $\tilde{\sigma}(L)$, it has been conjectured[5,22] that

$$\tilde{\sigma}(L)-\sigma_\perp \approx wL^{1-d}[\ln L + O(1)] \tag{2.15}$$

for periodic boundary conditions in general d, corresponding to

$$\xi_1 \propto L^w \exp(\sigma_\perp A) \tag{2.16}$$

where for $d=3$ the value of w may be different for $T>T_R^{(\perp)}$ and $T<T_R^{(\perp)}$. [Note that for $T<T_R^{(\perp)}$ the purely finite-size correction, as in (2.13), should

be exponentially small.] Relation (2.16) also applies for free boundary conditions in $d=2$ only. Exact Ising model calculations in $d=2$ yield[5,7,10,11]

$$w_{\text{periodic}}(2d) = 1/2 \tag{2.17}$$

$$w_{\text{free}}(2d) = 0 \tag{2.18}$$

The fact that the coefficient w in (2.15) differs from the coefficients of the $L^{1-d}\ln L$ terms in (2.13)–(2.14) is intriguing. It has been suggested[22] that an extra factor $\sim 1/\sqrt{A}$ enters in ξ_1 as a normalization of small fluctuations (distortions) about the lowest free energy intrinsic interfacial profile. However, intrinsic profile concepts can be defined unambiguously only in continuous mean-field-type theories.

3. TWO-DIMENSIONAL SYSTEMS WITH INTERFACES: CONTINUUM FORMULATION

In this section we begin our study of Ising-type systems with interfaces by first considering $L\times\infty$ strips in $d=2$. The $+-$ or *ap* boundary conditions force an interface in a system, running along the strip. For $+-$ boundary conditions, this is illustrated in Fig. 1. For the *ap* boundary conditions, the interface can wind around the strip, which has the topology of a cylindrical surface. As illustrated in Fig. 2, the transverse coordinate y must be considered mod$(2L)$. In both cases, one can use random-walk-type arguments to analyze the spectrum of the TM.[8,11] We consider such models in the next section. Here we will utilize a capillary-wave-type approach[23–25] to study the general features of the TM spectrum.

We assume that the orientation of the strip coincides with a symmetric lattice axis (which is typically the case in numerical applications[1]), such that the angle-dependent surface tension $\sigma(\theta)$, when measured per unit *projected* distance along the strip, has a quadratic minimum,[26]

$$\sigma(\theta)/\cos\theta = \tau + (1/2)\kappa\theta^2 + O(\theta^4) \tag{3.1}$$

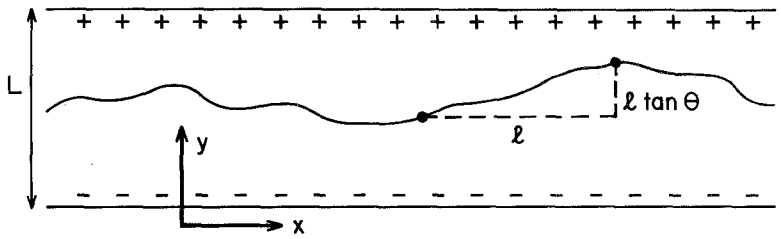

Fig. 1. Interface in an $L\times\infty$ Ising-type strip induced by the $+-$ boundary conditions. Other features shown are explained in the text (Section 3).

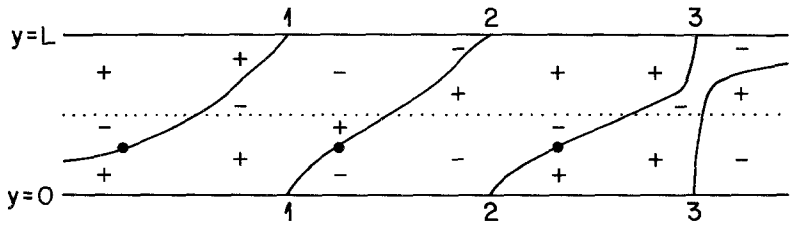

Fig. 2. Antiperiodic boundary conditions impose a mod($2L$) topology on a strip. Here the antiperiodic seam is shown in the middle (dotted line) for clarity. The interface winds periodically at the points marked 1, 2, 3. The three heavy-dotted points on the interface have the same y coordinate when measured in $0 \leqslant y \leqslant L$. However, *two windings* are required to reach an identical column configuration. The third (rightmost) winding at 3 illustrates a near-kink configuration: see text (Section 3).

with

$$\tau \equiv \sigma(0) > 0 \tag{3.2}$$

$$\kappa \equiv \sigma(0) + \sigma''(0) > 0 \tag{3.3}$$

These conventions are illustrated in Fig. 1, where a portion of the interface of projected length l and average inclination angle θ has been singled out. The free energy cost of this inclined interface is $k_B T\sigma(\theta)(l/\cos\theta)$. Thus, the surface tension per unit projected length (and per $k_B T$) is just the lhs of (3.1).[26] Note that the form (3.1) is characteristic of *rough interfaces* and thus applies for all $0 < T < T_c$ in $2d$. The quantity $\kappa = \kappa(T)$ is termed the *surface stiffness coefficient.*

In order to construct the effective TM for the longest scale correlations along the strip, let us consider the energy of a typical configuration depicted in Fig. 1. First, we note that the free energy $f(L)$ of the strip no longer converges exponentially to the bulk result [see (2.4)]. Indeed, for the *ap* boundary conditions it is well established[14] that

$$f_{ap}(L) - f(\infty) \approx \tau/L + O(e^{-L/\xi_\parallel}) \tag{3.4}$$

The added term, τ/L, represents the free energy contribution of the interface. For the $+-$ boundary conditions, we have

$$f_{+-}(L) - f(\infty) \approx (\tau + 2g)/L + \pi^2/(2\kappa L^3) + o(L^{-3}) \tag{3.5}$$

where we introduced free energy contributions g/L for each wall, as well as the leading capillary fluctuation contribution,[12,27,28] the form of which will be justified below. We remind the reader that various quantities here, τ, κ, g, etc., are implicitly T dependent.

In order to estimate the energy of the interfacial wandering or "fuzziness," we use the capillary wave approach.[23-25] In this coarse-grained description the interface is modeled by the single-valued function $y(x)$ (see Figs. 1 and 2). The Hamiltonian (in units of $k_B T$) in $2d$ is

$$H = \frac{\kappa}{2} \int_{x_{\min}}^{x_{\max}} dx[y'(x)]^2 + (x_{\max} - x_{\min})\, E \tag{3.6}$$

To have a finite free energy density, one must supplement (3.6) with cutoff prescriptions[23,24] and also allow for an additive regularizing term proportional to E in (3.6), where E is some cutoff and κ-dependent function.

Our aim is to identify the effective TM corresponding to (3.6). The detailed calculation is rather complicated and is not reproduced here. Instead, we first state the result and then offer arguments for its validity. The TM for (3.6) is approximately (see below) proportional to the differential operator

$$\hat{K} \equiv \exp\left(\frac{b}{2\kappa}\frac{d^2}{dy^2}\right) \tag{3.7}$$

For the $+-$ boundary conditions, $\hat{K}$ operates on functions $\psi(y)$ satisfying

$$\psi(L) = \psi(0) = 0 \tag{3.8}$$

where $0 \leqslant y \leqslant L$. For the *ap* boundary conditions, we have $0 \leqslant y \leqslant 2L$, and

$$\psi(2L) = \psi(0) \tag{3.9}$$

Thus, the eigenstates of $\hat{K}$, satisfying $\hat{K}\psi_n(y) = \lambda_n \psi_n(y)$, are given by

$$\psi_n^{(+-)} \propto \sin\frac{\pi n}{L} y, \qquad n = 1, 2, \ldots \tag{3.10}$$

$$\psi_n^{(ap)} \propto \exp\left(i\frac{\pi n}{L} y\right), \qquad n = 0, \pm 1, \pm 2, \ldots \tag{3.11}$$

In both cases

$$\lambda_n = \exp\left(-\frac{\pi^2 n^2 b}{2\kappa L^2}\right) \tag{3.12}$$

In order to substantiate the equivalence of $\hat{K}$ with the TM of (3.6), consider the case of unbounded y, i.e., disregard the details of the boundary effects. Then, for a slice of length b along the x axis, with the y values fixed at y_1 and y_2 at the ends, the capillary energy can be estimated by replacing

$$y' \to (y_2 - y_1)/b \tag{3.13}$$

Thus, we get $\Delta H(y_1, y_2) \simeq (\kappa/2b)(y_2 - y_1)^2 + bE$. After discretizing y in steps of, say, a, we can define the appropriate TM, with elements

$$e^{-bE} \exp\left[-\frac{\kappa}{2b} (y_2 - y_1)^2 \right] \tag{3.14}$$

However, the second factor here is just the diffusion kernel. Thus, in the continuous-y limit ($a \to 0$), one can employ the standard mathematical results[29] to prove that the "capillary" TM reduces to

$$\left(\frac{2\pi b}{\kappa a^2} \right)^{1/2} e^{-bE} \hat{K} \tag{3.15}$$

A more careful calculation (not detailed here) takes into account two previously neglected aspects of the problem. First, the approximation (3.13) must be improved to have the resulting kernel (3.14) consistent with the boundary effects. Second, the discreteness of the underlying lattice structure, i.e., the discretization of the x and y values in steps of b and a, respectively, makes the equivalence of the operator (3.15) with the lattice-model "capillary" TM approximate. The equivalence is restricted to a subspace of functions spanned by the eigenstates (3.10) or (3.11) corresponding to the largest eigenvalues: the precise condition is

$$n^2 \ll \min(\kappa L^2/b, L^2/a^2) \tag{3.16}$$

Thus, the correspondence becomes exact in the large-L limit.

The full effective TM of the *ap* boundary conditions can now be represented by the operator

$$C \exp\left[-bLf(\infty) - b\tau + \frac{b}{2\kappa} \frac{d^2}{dy^2} \right], \qquad (ap) \tag{3.17}$$

where we used (3.4). Here the coefficient $C \equiv (2\pi b/\kappa a^2)^{1/2} e^{-bE}$ remains to be determined. On physical grounds, however, one must select E to have

$$C \equiv 1 \tag{3.18}$$

to prevent the generation of $1/L$ terms in $f(L)$ beyond those in (3.4). Similarly, by examining (3.5), we arrive at the following effective TM for the $+-$ boundary conditions:

$$\exp\left[-bLf(\infty) - b(\tau + 2g) + \frac{b}{2\kappa} \frac{d^2}{dy^2} \right], \qquad (+-) \tag{3.19}$$

The operators (3.17) and (3.19) operate on functions satisfying (3.9) or (3.8), respectively.

For the largest TM eigenvalues in $2d$, we thus obtain the prediction

$$\Lambda_j^{(ap)} \approx \exp\left[-bLf(\infty) - b\tau - b\frac{\pi^2 j^2}{2\kappa L^2}\right] \tag{3.20}$$

where

$$j = 0, 1, 2, \ldots \ll \min(L(\kappa/b)^{1/2}, L/a) \tag{3.21}$$

and the eigenstates for $j > 0$ are doubly degenerate. Similarly,

$$\Lambda_j^{(+-)} \approx \exp\left[-bLf(\infty) - b(\tau + 2g) - b\frac{\pi^2(j+1)^2}{2\kappa L^2}\right] \tag{3.22}$$

where the j values are as in (3.21), and the eigenstates are all non-degenerate. For the leading correlation lengths we get

$$\xi_j^{(ap)} \approx \frac{2\kappa L^2}{\pi^2 j^2} \tag{3.23}$$

$$\xi_j^{(+-)} \approx \frac{2\kappa L^2}{\pi^2 j(j+2)} \tag{3.24}$$

where $j \geqslant 1$ is limited as in (3.21). The correlation lengths provide direct measures of the surface stiffness coefficient κ. Note that the $1/L^3$ term in (3.5) is also reproduced.

The algebraic behavior of the correlation lengths in $2d$ systems with interfaces has not been emphasized in the literature until recently.[7-11] One can raise the issue of why introducing transverse interfaces in addition to the longitudinal one should not be considered an important fluctuation yielding entropy gain without too much energy cost, as it is in the case of periodic boundary conditions. For the $+-$ boundary conditions, such a domain formation is very costly in energy since the phases near the walls are fixed. For the *ap* boundary conditions, the argument is more subtle, and is illustrated by the third winding (points 3) in Fig. 2. Such a rapid winding mimics the addition of a transverse interface on top of a smooth longitudinal interface. It is obvious, however, that the entropy can be gained with the investment of less bending energy, by more gradual windings.

4. TWO-DIMENSIONAL SYSTEMS: SOLID-ON-SOLID MODELS, AND SOME EXACT RESULTS

In this section we consider the TM spectrum of the solid-on-solid (SOS) models of interface fluctuations in $2d$ strips. These results serve to

check the continuum formalism of Section 3, and illustrate the pattern of corrections to (3.23)–(3.24). We also compare (3.23) for $j=1$ with the exact result[7,10,11] for the transverse Ising model.

The SOS modeling is essentially equivalent to the random walk arguments.[11] However, we use the *restricted* solid-on-solid (RSOS) model[20,30,31] (which finds further applications in the next section). We also outline the results for the *unrestricted* solid-on-solid (USOS) model[20,32,33] which is closer to the formulation of ref. 11.

The interface in the SOS approximation is described as a directed self-avoiding walk of $+\hat{x}$ and $\pm\hat{y}$ steps. Each $+\hat{x}$ step is of length b. The $\pm\hat{y}$ steps will be assumed to have length a. Let us assume that allowed x and y values are

$$x = bn, \qquad n = 0, \pm 1, \pm 2, \ldots \tag{4.1}$$

$$y = am, \qquad m = 1, 2, \ldots, L/a \tag{4.2}$$

For the RSOS model, at most one $+\hat{y}$ or $-\hat{y}$ step is allowed after each $+\hat{x}$ step. For the USOS model, several $+\hat{y}$ or several $-\hat{y}$ steps are possible at fixed x.

In the case of the $+-$ boundary conditions, the allowed y values are kept in the range (4.2). No $+\hat{y}$ steps are possible from $y=L$, and no $-\hat{y}$ steps are possible from $y=a$. For the *ap* boundary conditions, a unique labeling of configurations requires doubling the y range (see Fig. 2), i.e., $m=1, 2, \ldots, 2L/a$. The $+\hat{y}$ step from $y=2L$ ends at $y=a$, while the $-\hat{y}$ step from $y=a$ ends at $y=2L$. For the *ap* USOS case, the self-avoidance condition restricts the walk to have up to $(L/a-1)$ of the $+\hat{y}$ or $-\hat{y}$ steps at a given x.

We assign Boltzmann weights

$$u_\perp \qquad \text{for} \quad \pm\hat{y} \text{ steps} \tag{4.3}$$

$$u_\parallel \qquad \text{for} \quad +\hat{x} \text{ steps} \tag{4.4}$$

The SOS models approximate interfacial properties at low T of a rectangular-lattice $2d$ Ising model of spins ± 1 located at the x, y coordinates

$$x = b(n+1/2), \qquad n = 0, \pm 1, \pm 2, \ldots \tag{4.5}$$

$$y = a(m+1/2), \qquad m = 0, 1, \ldots, L/a \tag{4.6}$$

Thus, there are $L/a+1$ spins in each fixed-x column (connected by L/a bonds). For the $+-$ boundary conditions, the spins at $y=a/2$ are fixed at -1, the spins at $y=L+a/2$ are fixed at $+1$, while the spins in the remaining $L/a-1$ rows can take on any value (± 1). For the *ap* boundary

conditions, the spins in the L/a rows at $y = a/2, 3a/2, \ldots, L - a/2$ can fluctuate, while the spins at $y = L + a/2$ must assume minus the values of the spins at $y = a/2$, at the same x. The nearest neighbor ferromagnetic coupling constants along x and y, measured per $k_B T$, will be denoted by $K_x > 0$ and $K_y > 0$, respectively. For low T, the SOS approximation is obtained by identifying

$$u_\perp \equiv \exp(-2K_x) \tag{4.7}$$

$$u_\parallel \equiv \exp(-2K_y) \tag{4.8}$$

Thus,

$$0 < u_\parallel, u_\perp < 1 \tag{4.9}$$

The SOS models have been studied extensively in the literature.[20,30–33] For the RSOS case, we quote[20]

$$\tau_{\mathrm{RSOS}} = -\frac{1}{b} \ln[u_\parallel (1 + 2u_\perp)] \tag{4.10}$$

$$\kappa_{\mathrm{RSOS}} = \frac{b}{a^2} \left(\frac{1 + 2u_\perp}{2u_\perp} \right) \tag{4.11}$$

(Corresponding USOS results are also given in ref. 20.) Since these SOS models do not account for the free energy of the coexisting phases or for wall interactions, we use

$$f_{\mathrm{RSOS}}(\infty) = 0 \tag{4.12}$$

$$g_{\mathrm{RSOS}} = 0 \tag{4.13}$$

when comparing with the results of Section 3.

The TM formulation of the SOS models is well known. Specifically, the TM elements $t(m_1, m_2)$ for the RSOS model are given by

$$t(m, m) = u_\parallel \tag{4.14}$$

$$t(m, m \pm 1) = u_\parallel u_\perp \tag{4.15}$$

with all other TM elements vanishing. In (4.14)–(4.15), we take the index values $1, 2, \ldots, L/a$ for the $+-$ boundary conditions, but m is periodic mod$(2L/a)$ for the ap case. [Thus, (4.15) includes, e.g., $t(1, 2L/a) = u_\parallel u_\perp$, etc.] The eigenvalue equations

$$\sum_p t(m, p)\, \psi(p) = \Lambda \psi(m) \tag{4.16}$$

are solved by linear combinations of $\exp(\pm iqm)$, in fact, for all four SOS models mentioned here, i.e., RSOS or USOS, with $+-$ or ap. Specifically, we find

$$\psi_{\mathrm{RSOS}}^{(+-)}(m) \propto \sin qm \tag{4.17}$$

$$\psi_{\mathrm{RSOS}}^{(ap)}(m) \propto \exp(iqm) \tag{4.18}$$

with

$$\Lambda_{\mathrm{RSOS}} = u_{\parallel}(1 + 2u_{\perp} \cos q) \tag{4.19}$$

in both cases. The values of q are "quantized" as follows:

$$q_n^{(+-)} = n\pi a/(L+a), \qquad n = 1, 2, \ldots, L/a \tag{4.20}$$

$$q_n^{(ap)} = n\pi a/L, \qquad n = 0, \pm 1, \pm 2, \ldots, \pm(L-a)/a, +L/a \tag{4.21}$$

Note that all but the largest and the smallest eigenvalues ($n = 0$ and L/a) in the ap case are doubly degenerate.

Consider the small-q behavior, $\Lambda(q) = u_{\parallel}(1 + 2u_{\perp}) - u_{\parallel}u_{\perp}q^2 + O(q^4)$. By using (4.10)–(4.11), we can rearrange this expansion in the form

$$\Lambda(q) = \exp\left[-b\tau_{\mathrm{RSOS}} - \frac{bq^2}{2a^2\kappa_{\mathrm{RSOS}}} + O(q^4)\right] \tag{4.22}$$

With (4.12), (4.13), and (4.20), in which we assume $L \gg a$, and (4.21), it is evident that the general results (3.20), (3.22) for the largest TM eigenvalues are in fact confirmed for the RSOS model. The small-q expansion applies only to the largest RSOS eigenvalues, with the index n in (4.20)–(4.21) satisfying

$$|n| \ll L/a \tag{4.23}$$

This is consistent with (3.21), since

$$[L(\kappa/b)^{1/2}]_{\mathrm{RSOS}} = (L/a)[(1 + 2u_{\perp})/2u_{\perp}]^{1/2} > L/a \tag{4.24}$$

Finally, note that the $+-$ case eigenfunctions $\psi(m)$ given by (4.17) have the endpoint ($m = 1, L/a$) values

$$\psi(1) = \sin\left(\frac{n\pi a}{L+a}\right), \qquad \psi\left(\frac{L}{a}\right) = \sin\left(\frac{n\pi L}{L+a}\right) = (-1)^{n+1} \sin\left(\frac{n\pi a}{L+a}\right) \tag{4.25}$$

Thus, for n satisfying (4.23), the wave functions are vanishingly small at the endpoints: compare the "continuum" conditions (3.8).

We also worked out the detailed solution for the USOS model (not reported here). The new interesting features are as follows. The q dependence of $A(q)$ is modified as compared to (4.19), and in fact $A^{(+-)}(q)$ and $A^{(ap)}(q)$ are no longer identical, but differ in order $u_\perp^{L/a}$. The equal-space "quantization" of the q values, (4.20)–(4.21), is valid only up to corrections of order L^{-2} in q_n. The general predictions (3.20)–(3.22) are confirmed for the USOS model as well.

Consider now the full Ising spin model, with couplings K_x and K_y, as described above, without assuming the SOS approximation. One can consider the so-called "transverse Ising model" limit of extreme anisotropy,

$$K_x \to \infty, \qquad K_y \to 0 \tag{4.26}$$

with the fixed value of the parameter

$$\gamma \equiv K_y^{-1} \exp(-2K_x) \tag{4.27}$$

The Ising critical point is then fixed at $\gamma_c = 1$, with $\gamma < 1$ corresponding to $T < T_c$. For the leading spectral gap of the transverse Ising model, exact results have been reported,[7,9–11] which we "translate" to the correlation length. In the "transverse Ising model" literature, the (dimensionless) spectral gaps are considered, which are given by our $b(K_y \xi_j)^{-1}$. (This expression includes the exact proportionality factor.) Thus, in the limit $K_y \to 0$, with fixed γ,

$$\xi_1(L) \approx \frac{b(1-\gamma)\, L^2}{\pi^2 \gamma a^2 K_y} [1 + O(L^{-2})] \tag{4.28}$$

In order to check this against the general result (3.23), with $j = 1$, we quote the exact Ising model κ value,[20]

$$\kappa_{\text{Ising}} = \frac{b \sinh(b\tau_{\text{Ising}}) \sinh(2K_x)}{a^2 \sinh(2K_y)} \tag{4.29}$$

where[14]

$$\tau_{\text{Ising}} = \frac{1}{b} [2K_y + \ln(\tanh K_x)] \tag{4.30}$$

The limiting behaviors of these quantities are easily calculated,

$$\tau_{\text{Ising}} \approx 2K_y(1-\gamma)/b \tag{4.31}$$

$$\kappa_{\text{Ising}} \approx \frac{b(1-\gamma)}{2\gamma a^2 K_y} \tag{4.32}$$

Note that (4.31) should not be confused with the familiar limiting relation

$$(a\sigma_\perp)_{\text{Ising}} \equiv 2K_x + \ln(\tanh K_y) \approx -\ln \gamma \tag{4.33}$$

Finally, substituting (4.32) in the $j=1$ relation (3.23) reproduces the exact result (4.28).

5. THREE-DIMENSIONAL SYSTEMS BELOW THE ROUGHENING TEMPERATURE

In $d=3$, we add the z axis perpendicular to the xy plane (Fig. 1). For definiteness, we consider cylinders of rectangular cross section, $L \times M \times \infty$, where

$$0 \leqslant z \leqslant M \tag{5.1}$$

The $+-$ or *ap* boundary conditions are imposed in the y direction, as before, extended to all the allowed z values (5.1). In the z direction, we assume *periodic* boundary conditions, although we will mention the modifications required for free boundary conditions along z.

Below the roughening temperature, i.e., for fixed T in the range

$$0 < T < T_R \tag{5.2}$$

the interface will be microscopically flat on the average, over large distances, and parallel to the xz plane. The predominant fluctuations yielding entropy gain without too much energy cost will be steps (ledges) between different average y values. Upward $(+\hat{y})$ or downward $(-\hat{y})$ steps are equally probable; however, the average distance $\xi_1(L, M)$ between the steps will be exponentially large: see below.

We follow here the conventional "terrace-ledge" type model[12,34,35] of $3d$ interfaces for $T < T_R$. Obviously, there is no natural continuum limit here: the ledges are microscopic. Therefore, an underlying microscopic lattice structure must be introduced. For definiteness, we assume a *simple cubic* lattice model, with cubic axes along x, y, z. This choice is typical in numerical studies. However, it proves instructive to distinguish the lattice constant b along the x direction from that in the y direction, denoted by a.

Usually the step free energy s is defined[19] by imposing a tilt in an interface, induced by fixed boundary conditions in a large, approximately cubic sample. If the interface rises a distance Δy due to the tilt, then for $T < T_R$ it consists of terraces separated by $\Delta y/a$ steps (ledges). The free energy excess of the tilted interface, as compared to the free energy of a planar interface in the same sample, is proportional to Δy and also to the

length of the steps (M in our geometry). We define s as such an excessive free energy of a *single ledge*, i.e., $\Delta y = a$, measured per unit step length and per $k_B T$.

The above discussion suggests that the appropriate discrete model for the reduced TM for $T < T_R$ is the RSOS model (Section 4) with the Boltzmann weight for the $+\hat{x}$ steps replaced by

$$u_{\parallel} \to \exp[-bLM\tilde{f}(L, M)] \tag{5.3}$$

The weight for the $\pm\hat{y}$ steps is

$$u_{\perp} \to \exp[-M\tilde{s}(L, M)] \tag{5.4}$$

where

$$\lim_{L, M \to \infty} \tilde{s}(L, M) = s \tag{5.5}$$

and $\tilde{f}(L, M) \simeq f(L, M)$; see further below. Recall that we keep the cross-section shape fixed. Thus, the limits in (5.5) are taken with fixed L/M.

Before discussing the functions $\tilde{f}$ and $\tilde{s}$ entering (5.3)–(5.4) in detail, let us consider the implications of these relations. The weight for the transverse ($\pm\hat{y}$) steps $u_{\perp}$ is exponentially small in M. Note that the results for various SOS models (e.g., RSOS vs. USOS) typically differ only in $O(u_{\perp}^2)$. Thus, the simplest RSOS model is sufficiently general. Neglecting $O(u_{\perp}^2)$ corrections, we can replace relation (4.19) by

$$\Lambda(q) \simeq \exp\{-bLM\tilde{f}(L, M) + 2\cos q \exp[-M\tilde{s}(L, M)]\} \tag{5.6}$$

where we used (5.3), (5.4). Here q is "quantized" according to (4.20) or (4.21). Relation (5.6) should provide the correct asymptotic description not only for small q, but more generally for *all* the L/a or $2L/a$ (for $+-$ or *ap*, respectively) largest eigenvalues of the TM, forming a near degenerate multiplet as $L, M \to \infty$. Thus,

$$\Lambda_j^{(+-)} \approx \exp\left\{-bLM\tilde{f}(L, M) + 2\cos\left(\frac{\pi a(j+1)}{L+a}\right)\exp[-M\tilde{s}(L, M)]\right\} \tag{5.7}$$

where $j = 0, 1, \ldots, L/a - 1$, and

$$\Lambda_j^{(ap)} \approx \exp\left\{-bLM\tilde{f}(L, M) + 2\cos\left(\frac{\pi aj}{L}\right)\exp[-M\tilde{s}(L, M)]\right\} \tag{5.8}$$

where $j = 0, 1, 2, \ldots, L/a$, and the $j \neq 0$, L/a eigenvalues $\Lambda_j^{(ap)}$ are doubly degenerate.

Relations (5.7)–(5.8) with $j=0$ imply that interfacial fluctuations contribute only exponentially small terms to the cylinder free energy density for $T<T_R$, where

$$f(L, M) \equiv -(\ln \Lambda_0)/(bLM) \tag{5.9}$$

For the *ap* boundary conditions, a relation of the form (3.4) applies,

$$f_{ap}(L, M) - f(\infty, \infty) \approx \tau/L + O(e^{-L/\xi_\parallel}) + O(e^{-M/\xi_\perp}) \tag{5.10}$$

The step fluctuation contribution is essentially just one of the $O(e^{-M/\xi_\perp})$ type terms. The function $\tilde{f}(L, M)$ entering (5.3) and (5.8) can be formally defined by

$$\tilde{f}_{ap}(L, M) = f(L, M) + \frac{2}{bLM} \exp[-M\tilde{s}(L, M)] \tag{5.11}$$

However, the consideration of its detailed size dependences is no more useful than that for $f(L, M)$. A similar line of argument applies for the $+-$ boundary conditions, where the wall free energy must be included in (5.10) [see (3.5)]. For both boundary conditions along y, if we change the z boundary conditions from periodic to free, additional $1/M$ wall as well as $1/(LM)$ edge terms (for $+-$ along y) will enter.

We now turn to the issue of the convergence rate in (5.5). The fluctuations of the "dilute gas" of steps of length M (along the z direction) are reminiscent of the dilute gas of interfaces in $2d$ (Section 2). Therefore, a relation of the type (2.15) should apply,

$$\tilde{s}(L, M) - s \approx wM^{-1}[\ln M + O(1)] \tag{5.12}$$

and it is tempting to conjecture that the w values are identical to those in (2.17)–(2.18) for the periodic ($w=1/2$) and free ($w=0$) boundary conditions along z. However, such a conjecture requires numerical tests: We will keep w general. Thus, we substitute in (5.7)–(5.8)

$$\exp[-M\tilde{s}(L, M)] \to \mu^{-1}M^{-w} \exp(-Ms) \tag{5.13}$$

where μ is some T-dependent function of dimensions (length)$^{-w}$, which may also depend on the boundary conditions along z. (Similarity of finite-size effects for fluctuating steps in $3d$ with interfaces in $2d$ has been explored in a different context in ref. 36.)

For the leading finite-size correlation lengths, we get

$$\xi_j^{(+-)}(L, M) \approx b\mu M^w e^{Ms} \left[\sin \frac{\pi a(j+2)}{2(L+a)} \sin \frac{\pi aj}{2(L+a)} \right]^{-1} \tag{5.14}$$

where $j = 1,..., L/a - 1$, and

$$\xi_j^{(ap)}(L, M) \approx b\mu M^w e^{Ms} \left(\sin \frac{\pi aj}{2L} \right)^{-2} \tag{5.15}$$

where $j = 1,..., L/a$. For the longest correlations, one can further expand

$$\xi_{j \ll L/a}^{(+-)} \approx \frac{4b\mu L^2 M^w \exp(Ms)}{\pi^2 a^2 j(j+2)} \tag{5.16}$$

$$\xi_{j \ll L/a}^{(ap)} \approx \frac{4b\mu L^2 M^w \exp(Ms)}{\pi^2 a^2 j^2} \tag{5.17}$$

The leading correlation lengths provide direct measures of the single-step free energy s for fixed $0 < T < T_R$. Recall that $\mu(T)$ and w depend on the boundary conditions along z, and it is likely that for the periodic and free cases we have $w = 1/2$ and 0, respectively. Finally, note that the absence of a continuum limit here is seen explicitly in that the lattice spacings a and b enter (5.11) and (5.14)–(5.17).

6. THREE-DIMENSIONAL SYSTEMS ABOVE THE ROUGHENING TEMPERATURE. CONCLUDING REMARKS

For $3d$ systems with T fixed in

$$T_R < T < T_c \tag{6.1}$$

the interface is rough, i.e., strongly fluctuating. As in the $d = 2$ case, we will assume that the cylinder is oriented symmetrically with respect to the underlying lattice structure, in such a way that the surface tension (free energy per unit interfacial area and per $k_B T$), when considered per projected area, has a parabolic (quadratic) minimum with respect to arbitrary inclinations. Two-angle parametrization of inclinations in $3d$, selection of the principal axes, and the concept of the principal stiffness coefficients κ_1 and κ_2, etc., have been discussed, e.g., in ref. 19. For our purposes here it is sufficient to quote that for inclinations that keep the interface perpendicular to the xy plane, and which are therefore specified by one angle θ, relations (3.1)–(3.3) apply.[19]

The longest wavelength capillary modes, setting the largest length scales $\xi_j(L, M)$, "propagate" along the cylinder axis. These fluctuations correspond to interfaces remaining on the average flat and parallel to the z axis in the cross section, but with a slowly varying y coordinate. Thus, the relevant modes are essentially the same as in the $2d$ case, with the *effective stiffness* $M\kappa$. (Note that the units of this product are those of κ in $2d$.) We therefore conclude that for the $3d$ Ising-type systems at $T_R < T < T_c$,

$$\xi_j^{(ap)} \approx \frac{2\kappa ML^2}{\pi^2 j^2} \tag{6.2}$$

$$\xi_j^{(+-)} \approx \frac{2\kappa ML^2}{\pi^2 j(j+2)} \tag{6.3}$$

for

$$j = 1, 2, \ldots \ll L/a \tag{6.4}$$

where we used (3.23)–(3.24).

If the boundary conditions in the z direction are periodic, detailed predictions also can be made for the cylinder free energy. We only quote the results here,

$$f_{ap}(L, M) \approx f(\infty, \infty) + \tau/L \tag{6.5}$$

$$f_{+-}(L, M) \approx f(\infty, \infty) + (\tau + 2g)/L + \pi^2/(2\kappa M^2 L^3) \tag{6.6}$$

In summary, we preseted detailed theoretical predictions for the largest TM eigenvalues in the $2d$ and $3d$ cylinder geometries with interfaces. It is hoped that our formulas will be useful in numerical calculations of $\kappa(T)$ and $s(T)$. Several topics have not been addressed here. These include scaling forms near T_c and T_R, as well as studies of more complicated boundary conditions, of the type considered in refs. 7–11. Little is known about the global structure of the TM spectrum for systems with interfaces and on the development of bulk correlations in the $L \to \infty$ limit.

ACKNOWLEDGMENTS

This research has been supported by the U.S. National Science Foundation under grant DMR-86-01208 and by the Donors of the Petroleum Research Fund, administered by the American Chemical Society, under grant ACS-PRF-18175-G6. This financial assistance is gratefully acknowledged.

REFERENCES

1. M. P. Nightingale, *J. Appl. Phys.* **53**:7927 (1982).
2. C. J. Hamer and C. H. J. Johnson, *J. Phys. A* **19**:423 (1986).
3. H. Saleur and B. Derrida, *J. Phys.* (Paris) **46**:1043 (1985).
4. M. E. Fisher, *J. Phys. Soc. Jpn.* (Suppl.) **26**:87 (1969).
5. V. Privman and M. E. Fisher, *J. Stat. Phys.* **33**:385 (1983).
6. M. E. Fisher and V. Privman, *Phys. Rev. B* **32**:447 (1985).
7. G. G. Cabrera and R. Jullien, *Phys. Rev. Lett.* **57**:393 (1986).
8. J. Zinn-Justin, *Phys. Rev. Lett.* **57**:3296 (1986).
9. G. G. Cabrera and R. Jullien, *Phys. Rev. Lett.* **57**:3297 (1986).
10. G. G. Cabrera and R. Jullien, *Phys. Rev. B* **35**:7062 (1987).
11. M. N. Barber and M. E. Cates, *Phys. Rev. B* **36**:2024 (1987).
12. H. van Beijeren and I. Nolden, in *Structure and Dynamics of Surfaces II*, W. Schommers and P. van Blanckenhagen, eds. (Springer-Verlag, Berlin, 1987), and references therein.
13. M. E. Fisher, in *Critical Phenomena, Proceedings 1970 Enrico Fermi International School of Physics*, Vol. 51, M. S. Green, ed. (Academic Press, New York, 1971).
14. L. Onsager, *Phys. Rev.* **65**:117 (1944).
15. V. Privman and L. S. Schulman, *J. Stat. Phys.* **29**:205 (1982), and references therein.
16. D. B. Abraham, *Stud. Appl. Math.* **50**:71 (1971).
17. C. Domb, *Adv. Phys.* **9**:149 (1960); esp. Section 3.5.1(v).
18. M. P. Gelfand and M. E. Fisher, *Int. J. Thermophys.* (1989), in print.
19. V. Privman, *Phys. Rev. Lett.* **61**:183 (1988).
20. N. M. Švrakić, V. Privman, and D. B. Abraham, *J. Stat. Phys.* **53**:1041 (1988).
21. N. J. Gunter, D. A. Nicole, and D. J. Wallace, *J. Phys. A* **13**:1755 (1980).
22. E. Brézin and J. Zinn-Justin, *Nucl. Phys. B* **257**[FS14]:867 (1985).
23. F. P. Buff, R. A. Lovett, and F. H. Stillinger, Jr., *Phys. Rev. Lett.* **15**:621 (1965).
24. J. D. Weeks, *J. Chem. Phys.* **67**:3106 (1977).
25. D. S. Fisher and J. D. Weeks, *Phys. Rev. Lett.* **50**:1077 (1983).
26. M. P. A. Fisher, D. S. Fisher, and J. D. Weeks, *Phys. Rev. Lett.* **48**:368 (1982).
27. M. E. Fisher and D. S. Fisher, *Phys. Rev. B* **25**:3192 (1982).
28. J. Bricmont, A. El Mellouki, and J. Fröhlich, *J. Stat. Phys.* **42**:743 (1986).
29. M. Kac, in *Brandeis Lectures 1966*, Vol. 1, M. Chretien, E. P. Gross, and S. Deser, eds. (Gordon and Breach, New York, 1968).
30. S. T. Chui and J. D. Weeks, *Phys. Rev. B* **23**:2438 (1981).
31. V. Privman and N. M. Švrakić, *Phys. Rev. B* **37**:3713 (1988).
32. H. N. V. Temperley, *Proc. Camb. Phil. Soc.* **48**:683 (1952).
33. V. Privman and N. M. Švrakić, *J. Stat. Phys.* **51**:1111 (1988), and references therein.
34. E. E. Gruber and W. W. Mullins, *J. Phys. Chem. Solids* **28**:875 (1967).
35. C. Jayaprakash, C. Rottman, and W. F. Saam, *Phys. Rev. B* **30**:6549 (1984).
36. M. P. Gelfand, to be published.